

Anion-directed assembly: Framework conversion in dimensionality and photoluminescence

Yun Gong^{a,b}, Tianfu Liu^a, Wang Tang^a, Fengjing Wu^b, Wenliang Gao^b, Changwen Hu^{a,*}

^aDepartment of Chemistry, Beijing Institute of Technology, Beijing 100081, PR China

^bDepartment of Chemistry, College of Chemistry and Chemical Engineering, Chongqing University, Chongqing 400044, PR China

Received 17 September 2006; received in revised form 18 January 2007; accepted 24 January 2007

Available online 16 February 2007

Abstract

Six novel Ni(II)-fluconazole complexes formulated as $(C_{13}H_{11}N_6OF_2)_2Ni_2(NO_3)_2$ (**1**), $(C_{13}H_{12}N_6OF_2)_2Ni(NO_3)_2 \cdot H_2O$ (**2**), $(C_{13}H_{12}N_6OF_2)Ni(SO_4)(DMF)_2(H_2O)$ (**3**), $(C_{13}H_{12}N_6OF_2)_2Ni(H_2O)_2(SO_4) \cdot 4H_2O$ (**4**), $(C_{13}H_{12}N_6OF_2)_2NiCl_2 \cdot 2(CH_3OH)$ (**5**), $(C_{13}H_{12}N_6OF_2)_4Ni_2(MoO_4)_2 \cdot 6H_2O$ (**6**) have been hydrothermally or solvothermally synthesized under similar conditions except different anions and solvents. They are structurally characterized by elemental analysis, IR, TG and single crystal X-ray diffraction. Complex **1** is a molecular binuclear nickel cluster. Complex **2** exhibits a one-dimensional (1D) chain linked by double-stranded fluconazole-bridge. Complex **3** shows a novel 1D chain linked by double-stranded fluconazole-bridge and double-stranded SO_4^{2-} -bridge. Complex **4** shows a three-dimensional (3D) architecture and SO_4^{2-} anions occupy the cavity. Complex **5** exhibits a two-dimensional (2D) structure constructed by alternating left- and right-handed helices. Complex **6** exhibits a 3D architecture, in which the 2D layers are pillared by $\{MoO_4\}$ tetrahedra. Complex **2** can be irreversibly converted to complex **1** in the presence of DMF (*N,N*-dimethylformamide). Complexes **1**, **3** and **6** show antiferromagnetic interactions between the nickel (II) ions. The photoluminescence properties of the six complexes indicated that the introduction of different anions can enhance or weaken the intra-ligand transitions of fluconazole.

© 2007 Elsevier Inc. All rights reserved.

Keywords: Fluconazole; Anion; Solvent; Self-assembly; Photoluminescence

1. Introduction

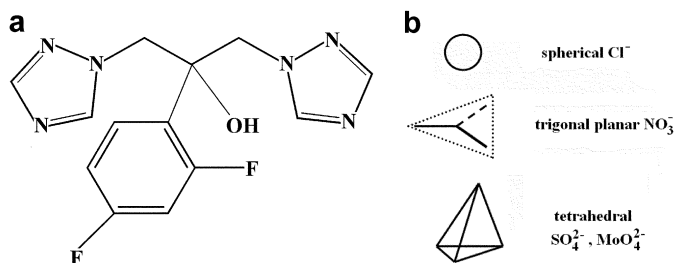
Anion binding and recognition have received much attention, because of its importance in biological and chemical processes [1–2]. Many enzyme reactions involve the selective transformation of anions [1]. The selective extraction of anionic pollutants also requires the development of specific coordination sites [2a]. Anion-directed self-assembly is an important field in anion coordination chemistry [3]. However, rational design of anion-assisted self-assembly processes is particularly challenging compared with to the analogous studies involving cationic and neutral species [4], which is attributed to some of the intrinsic properties of anions such as their diffuse nature (small charge to radius ratio), pH sensitivity, and

their relative high solvation free energies [5]. Based on the principle of electroneutrality that all pure substances fulfill, in the crystalline phase all positive charges must be compensated by negative counter charges, either the positive charge on the metal center is balanced by the negative charge on the organic ligand or if this was not the case, a third anionic component would be required. In an attempt to rationalize the effect of the counteranion upon the self-assembly, our strategy is to choose a neutral organic ligand which has a tendency to form metal complexes.

Fluconazole, a good antifungal agent in the treatment of candidiasis [6] first seized our attention based on the following considerations: (a) from the view of biological importance, the interaction between metal ions with drugs is a subject of great interest [7]. In some cases, the highest activity of drug is associated with a metal atom [8]. (b) Two 1,2,4-triazole ligands of fluconazole (Scheme 1a) can

*Corresponding author. Fax: +86 23 6282 8869.

E-mail address: cwhu@bit.edu.cn (C. Hu).



Scheme 1. The structure of fluconazole (a) and the geometrical configuration of anions (b).

combine metal ions in their neutral form and anion must be incorporated into the metal complexes for the balance of charge. (c) Three carbon atoms bridge the two triazole ligands and the flexible C–C chain of fluconazole can be rotated for suitable position and angle to fit the size and geometrical configuration of anions in the self-assembly of metal complexes. (d) The big substituent, 2,4-difluorophenyl, can avoid the interpenetration due to steric hindrance at metal center when fluconazole binds to metal ion.

In the present work, we choose four kinds of ordinary anions with different sizes and geometrical configurations, that is, spherical Cl^- , trigonal planar NO_3^- , tetrahedral SO_4^{2-} and MoO_4^{2-} (Scheme 1b). It is reported the syntheses, characterization and conversion of a series of Ni(II)–fluconazole complexes under similar reaction conditions (including the same temperature, time and metal-to-ligand ratio) except different counteranions. During the synthesis, due to the pH sensitivity of anions, no acid or base was added into the reaction mixtures. We change the species of solvents for suitable single crystals. Their thermogravimetric analysis and photoluminescence properties have been investigated. The magnetic characteristics of complexes **1**, **3** and **6** have been explored.

2. Experimental section

2.1. General considerations

All chemicals purchased were of reagent grade and used without further purification. Fluconazole was supplied by Chongqing care life pharmaceutical limited company. C, H, N elemental analyses were performed on Perkin–Elmer 240c elemental analyzer. Infrared spectra were recorded as KBr pellets on a Nicolet 170SXFT/IR spectrometer. TG analyses were carried out in air between 20 and 1000 °C at a heating rate of 10 °C min⁻¹ on a NETZSCH STA 449 °C simultaneous thermal analyzer. The magnetic susceptibility data were recorded over the 2–300 K temperature range using a Quantum Design MPMS-5S SQUID susceptibility meter. X-ray powder diffraction (XRD) of samples were collected on a Japan Rigaku D/max γ A X-ray diffractometer equipped with graphite monochromatized $\text{CuK}\alpha$ radiation ($\lambda = 0.154060$ nm). The 2θ range used was from 5° to 40° in steps of 0.04° with a count time 1 s. Excitation and emission spectra were obtained on an RF-5301PC

spectrofluorometer equipped with a 450W xenon lamp as the excitation source. All measurements were performed at room temperature.

2.2. Synthesis

$(\text{C}_{13}\text{H}_{11}\text{N}_6\text{OF}_2)_2\text{Ni}_2(\text{NO}_3)_2$ (**1**): A mixture of $\text{Ni}(\text{NO}_3)_2 \cdot 6\text{H}_2\text{O}$ (0.5 mmol, 0.146 g), fluconazole (0.5 mmol, 0.153 g) and DMF (*N,N'*-dimethylformamide) (10 mL) was sealed in a Teflon-lined autoclave and heated at 110 °C for three days, then followed by slow cooling to room temperature. The resulting green crystals were filtered off and washed with DMF (yield: ca. 95% based on fluconazole). Elemental Anal. Found: C, 36.78; H, 2.66; N, 23.18%. Calcd. for $\text{C}_{26}\text{N}_{14}\text{H}_{22}\text{Ni}_2\text{O}_8\text{F}_4$: C, 36.62; H, 2.58; N, 23.00%. IR (cm^{-1}): 3419(m), 3111(m), 1619(m), 1497(s), 1386(s), 1288(s), 1151(s), 1058(m), 958(s), 870(m), 673(m), 656(m).

$(\text{C}_{13}\text{H}_{12}\text{N}_6\text{OF}_2)_2\text{Ni}(\text{NO}_3)_2 \cdot \text{H}_2\text{O}$ (**2**): The preparation of complex **2** was similar to that of complex **1** except using water instead of DMF. Yield: ca. 95% based on fluconazole. Elemental Anal. Found: C, 38.49; H, 3.12; N, 24.32%. Calcd. for $\text{C}_{26}\text{N}_{14}\text{H}_{26}\text{NiO}_9\text{F}_4$: C, 38.38; H, 3.20; N, 24.11%. IR (cm^{-1}): 3331(m), 3136(m), 1622(m), 1504(s), 1352(s), 1284(s), 1130(s), 1053(m), 962(s), 867(m), 678(m), 663(m).

$(\text{C}_{13}\text{H}_{12}\text{N}_6\text{OF}_2)_2\text{Ni}(\text{SO}_4)(\text{DMF})_2(\text{H}_2\text{O})$ (**3**): The preparation of complex **3** was similar to that of complex **1** except using NiSO_4 (0.5 mmol, 0.131 g) instead of $\text{Ni}(\text{NO}_3)_2 \cdot 6\text{H}_2\text{O}$. Yield: ca. 90% based on fluconazole. Elemental Anal. Found: C, 36.59; H, 4.52; N, 17.78%. Calcd. for $\text{C}_{19}\text{N}_8\text{H}_{28}\text{NiO}_8\text{F}_2\text{S}$: C, 36.48; H, 4.48; N, 17.92%. IR (cm^{-1}): 3128(s), 1660(s), 1530(s), 1504 (s), 1421(s), 1383(s), 1288(s), 1084(s), 967(m), 859(m), 680(m), 661(m).

$(\text{C}_{13}\text{H}_{12}\text{N}_6\text{OF}_2)_2\text{Ni}(\text{H}_2\text{O})_2(\text{SO}_4) \cdot 4\text{H}_2\text{O}$ (**4**): The preparation of complex **4** was similar to that of complex **3** except using water instead of DMF. Yield: ca. 90% based on fluconazole. Elemental Anal. Found: C, 35.59; H, 4.02; N, 19.01%. Calcd. for $\text{C}_{26}\text{N}_{12}\text{H}_{36}\text{NiO}_{12}\text{F}_4\text{S}$: C, 35.66; H, 4.11; N, 19.20%. IR (cm^{-1}): 3159(s), 1619(s), 1533(s), 1498(s), 1426(s), 1375(m), 1290(s), 1153(s), 1036(s), 967(m), 852(m), 671(s).

$(\text{C}_{13}\text{H}_{12}\text{N}_6\text{OF}_2)_2\text{NiCl}_2 \cdot 2(\text{CH}_3\text{OH})$ (**5**): The synthesis of complex **5** was carried out as described above for complex **1**, but starting with $\text{NiCl}_2 \cdot 6\text{H}_2\text{O}$ (0.5 mmol, 0.119 g) and methanol instead of $\text{Ni}(\text{NO}_3)_2 \cdot 6\text{H}_2\text{O}$ and DMF. Yield: ca. 90% based on fluconazole. Elemental Anal. Found: C, 41.79; H, 4.02; N, 20.61%. Calcd. for $\text{C}_{28}\text{N}_{12}\text{H}_{32}\text{NiO}_4\text{F}_4\text{Cl}_2$: C, 41.58; H, 3.96; N, 20.79%. IR (cm^{-1}): 3257(s), 1620(s), 1522(s), 1499(s), 1418(s), 1279(s), 1128(s), 1086(m), 968(m), 675(s).

$(\text{C}_{13}\text{H}_{12}\text{N}_6\text{OF}_2)_4\text{Ni}_2(\text{MoO}_4)_2 \cdot 6\text{H}_2\text{O}$ (**6**): The synthesis of complex **6** was carried out as described above for complex **1**, but starting with the mixture of $\text{NiCl}_2 \cdot 6\text{H}_2\text{O}$ (0.5 mmol, 0.119 g), $\text{Na}_2\text{MoO}_4 \cdot 2\text{H}_2\text{O}$ (1 mmol, 0.242 g), fluconazole (0.5 mmol, 0.153 g) and water (10 mL). Yield: ca. 60% based on fluconazole. Elemental Anal. Found: C, 35.51; H, 3.12; N, 18.66%. Calcd. for $\text{C}_{52}\text{N}_{24}\text{H}_{60}\text{Ni}_2\text{O}_{18}\text{F}_8\text{Mo}_2$: C,

35.25; H, 3.39; N, 18.98%. IR(cm^{-1}): 3384(s), 3104(s), 1618(s), 1524(s), 1499(s), 1426(s), 1285(s), 1139(s), 1112(m), 839(s), 659(m).

2.3. Crystallographic studies

XRD data of complexes **1–6** were collected on a Bruker-AXS CCD area detector-equipped diffractometer with graphite-monochromatized $\text{MoK}\alpha$ ($\lambda = 0.71073 \text{ \AA}$) radiation at room temperature. A total of 19,676 (3892 unique, $R_{\text{int}} = 0.0302$) reflections of complex **1** ($-9 \leq h \leq 17$, $-18 \leq k \leq 16$, $-22 \leq l \leq 21$, $2.38 < \theta < 28.27$), a total of 8183 (2917 unique, $R_{\text{int}} = 0.0455$) reflections of **2** ($-11 \leq h \leq 12$, $-18 \leq k \leq 14$, $-24 \leq l \leq 23$, $1.95 < \theta < 25.01$), a total of 14081 (4787 unique, $R_{\text{int}} = 0.0607$) reflections of **3** ($-11 \leq h \leq 15$, $-12 \leq k \leq 16$, $-17 \leq l \leq 16$, $2.00 < \theta < 25.01$), a total of 19,039 (6482 unique, $R_{\text{int}} = 0.0301$) reflections of **4** ($-15 \leq h \leq 18$, $-21 \leq k \leq 21$, $-13 \leq l \leq 15$, $1.95 < \theta < 25.01$), a total of 9121 (3173 unique, $R_{\text{int}} = 0.0381$) reflections of **5** ($-25 \leq h \leq 27$, $-11 \leq k \leq 10$, $-23 \leq l \leq 22$, $2.11 < \theta < 25.01$), a total of 11208 (4209 unique, $R_{\text{int}} = 0.0284$) reflections of **6** ($-20 \leq h \leq 24$, $-21 \leq k \leq 21$, $-17 \leq l \leq 17$, $1.80 < \theta < 28.36$) were measured. An empirical absorption correction from ψ scan was applied. All the structures were solved by direct methods and expanded using Fourier techniques. The nonhydrogen atoms were refined anisotropically. All of the hydrogen atoms were placed in the calculated positions. All calculations were performed using the SHELXTL-97 program. The CCDC reference numbers are the following: 297,388 for complex **1**, 297,389 for complex **2**, 297,392 for complex **3**, 297,393 for complex **4**, 297,390 for complex **5**, 297,391 for complex **6**. Crystal data and structure refinements for compounds **1–6** are listed in Table 1. Selected bond lengths and angles for compounds **1–6** are listed in Tables 2–7. Further details are provided in the Supporting Information.

3. Results and discussion

3.1. Synthesis

Hydrothermal or solvothermal synthesis has recently been proved a useful technique in preparation of crystalline inorganic–organic hybrids. In our case, compounds **1–6** were prepared by such method. Under such conditions, the different solubilities of the organic and inorganic starting materials are alleviated. The hydrothermal or solvothermal temperature (below 200°C) avoids decomposition of organic components and promotes “self-assembly” of crystalline metastable phases from simple molecular precursors.

In the present work, the preparations of compounds **1–6** were not susceptible to the reaction temperature and reaction time. In general, solutions of fluconazole and metal salt were treated hydrothermally or solvothermally for 2–3 days at temperatures of $110\text{--}180^\circ\text{C}$ to produce

Table 1
Crystal data and structure refinements for complexes **1–6**

Compound	1	2	3	4	5	6
Formula	$\text{C}_{26}\text{N}_{14}\text{H}_{22}\text{Ni}_2\text{O}_8\text{F}_4$	$\text{C}_{26}\text{N}_{14}\text{H}_{26}\text{NiO}_6\text{F}_4$	$\text{C}_{19}\text{N}_8\text{H}_{28}\text{NiO}_8\text{F}_2\text{S}$	$\text{C}_{26}\text{N}_{12}\text{H}_{36}\text{NiO}_{12}\text{F}_4\text{S}$	$\text{C}_{28}\text{N}_{12}\text{H}_{32}\text{NiO}_4\text{F}_4\text{Cl}_2$	$\text{C}_{52}\text{N}_{24}\text{H}_{60}\text{Ni}_2\text{O}_{18}\text{F}_8\text{Mo}_2$
<i>M</i>	852	813	625	875	806	1767
Crystal system	Orthorhombic	Monoclinic	Monoclinic	Monoclinic	Monoclinic	Monoclinic
Space group	<i>Pbca</i>	<i>C2/c</i>	<i>P2_1/c</i>	<i>P2_1/c</i>	<i>C2/c</i>	<i>C2/c</i>
<i>a</i> (Å)	13.524(2)	10.356(13)	13.010(3)	15.896(2)	22.818(5)	18.077(3)
<i>b</i> (Å)	13.686(2)	15.39(2)	14.128(4)	17.992(3)	9.288(2)	16.392(3)
<i>c</i> (Å)	17.103(3)	20.85(3)	14.865(4)	12.928(2)	20.156(4)	13.495(2)
α (deg)	90	90	90	90	90	90
β (deg)	90	91.26(2)	96.801(4)	96.206(2)	122.317(3)	120.546(2)
γ (deg)	90	90	90	90	90	90
<i>V</i> (Å ³)	3165.6(9)	3321(7)	2713.2(12)	3675.5(10)	3609.9(13)	3444.1(9)
<i>Z</i>	4	4	4	4	4	2
ρ_{calc} (g cm^{-3})	1.788	1.626	1.531	1.582	1.484	1.703
μ (mm^{-1})	1.288	0.681	0.864	0.681	0.758	1.001
<i>F</i> (000)	1728	1664	1296	1808	1656	1784
Goodness-of-fit on F^2	1.060	1.032	1.018	1.023	1.034	0.954
Final <i>R</i> indices [$I > 2\sigma(I)$]	$R_1 = 0.0310$, $wR_2 = 0.0756$	$R_1 = 0.0570$, $wR_2 = 0.1441$	$R_1 = 0.0520$, $wR_2 = 0.1193$	$R_1 = 0.0365$, $wR_2 = 0.0870$	$R_1 = 0.0445$, $wR_2 = 0.1022$	$R_1 = 0.0397$, $wR_2 = 0.0949$
<i>R</i> indices (all data)	$R_1 = 0.0530$, $wR_2 = 0.0872$	$R_1 = 0.0767$, $wR_2 = 0.1545$	$R_1 = 0.1066$, $wR_2 = 0.1536$	$R_1 = 0.0643$, $wR_2 = 0.1228$	$R_1 = 0.0780$, $wR_2 = 0.1228$	$R_1 = 0.0625$, $wR_2 = 0.1126$

$$R_1 = \frac{\sum ||F_o| - |F_c||}{\sum |F_o|}, wR_2 = \frac{\sum [w(F_o^2 - F_c^2)^2]}{\sum [w(F_o^2)]^{1/2}}$$

Table 2
Selected bond lengths (Å) and angles (deg) for complex 1

<i>Bond lengths</i>			
Ni(1)–O(1)#1	2.0160(14)	Ni(1)–O(1)	2.0242(13)
Ni(1)–N(2)	2.051(2)	Ni(1)–N(5)#1	2.0573(19)
Ni(1)–O(2)	2.1261(16)	Ni(1)–O(3)	2.1548(18)
<i>Bond angles</i>			
O(1)#1–Ni(1)–O(1)	82.06(6)	O(1)#1–Ni(1)–N(2)	98.92(7)
O(1)–Ni(1)–N(5)#1	170.52(7)	O(1)#1–Ni(1)–O(2)	159.62(7)
N(2)–Ni(1)–N(5)#1	93.69(8)	O(2)–Ni(1)–O(3)	60.45(7)
C(4)–N(2)–Ni(1)	136.57(17)	N(1)–N(2)–Ni(1)	118.63(14)
N(2)–Ni(1)–O(3)	160.84(7)	C(6)–N(5)–Ni(1)#1	136.24(18)

Symmetry transformations used to generate equivalent atoms: #1 $-x + 1, -y + 2, -z + 1$.

Table 3
Selected bond lengths (Å) and angles (deg) for complex 2

<i>Bond lengths</i>			
Ni(1)–N(6)#1	2.024(4)	Ni(1)–N(6)	2.024(4)
Ni(1)–N(3)	2.026(4)	Ni(1)–N(3)#1	2.026(4)
Ni(1)–O(2)	2.427(4)	Ni(1)–O(2) #1	2.427(4)
<i>Bond angles</i>			
N(6)#1–Ni(1)–N(6)	180.00(16)	N(6)#1–Ni(1)–N(3)	90.43(15)
N(6)–Ni(1)–O(2)	87.65(17)	N(3)#1–Ni(1)–O(2)	91.91(15)
N(3)–Ni(1)–O(2)	88.09(15)	N(6)#1–Ni(1)–N(3)#1	89.57(15)
C(2)–N(3)–Ni(1)	126.6(3)	C(1)–N(3)–Ni(1)	131.1(3)
N(7)–O(2)–Ni(1)	148.8(3)	O(1)–C(4)–C(5)#2	109.2(3)

Symmetry transformations used to generate equivalent atoms: #1 $-x + 1/2, -y + 3/2, -z + 1$; #2 $-x + 3/2, -y + 3/2, -z + 1$.

Table 4
Selected bond lengths (Å) and angles (deg) for complex 3

<i>Bond lengths</i>			
Ni(1)–O(2)	2.065(3)	Ni(1)–N(3)	2.081(4)
Ni(1)–O(6)	2.087(4)	Ni(1)–O(3)#1	2.089(3)
Ni(1)–O(7)	2.091(3)	Ni(1)–N(6)#2	2.094(4)
<i>Bond angles</i>			
O(2)–Ni(1)–N(3)	88.80(15)	O(2)–Ni(1)–O(6)	174.30(15)
O(7)–Ni(1)–N(6)#2	177.12(15)	N(3)–Ni(1)–O(6)	85.50(16)
N(3)–Ni(1)–O(3)#1	175.88(15)	N(3)–Ni(1)–O(7)	87.37(15)
C(4)–N(3)–Ni(1)	126.0(3)	S(1)–O(2)–Ni(1)	138.0(2)
C(5)–N(3)–Ni(1)	131.5(4)	S(1)–O(3)–Ni(1)#1	134.7(2)

Symmetry transformations used to generate equivalent atoms: #1 $-x, -y + 1, -z$; #2 $-x, -y + 1, -z + 1$.

crystalline products in good yields (90–95% for complexes 1–5 and 60% for complex 6).

The preparations of compounds 1–5 were not susceptible to the molar ratios of reactants. Compounds 1–5 can be obtained upon the 1:1 or 2:1 mol ratio of Ni(II)/fluconazole. As well known, the 1:1 mol ratio of Ni(II)/fluconazole represents 1:1 mol ratio of SO_4^{2-} /fluconazole and 2:1 mol ratio of NO_3^- (or Cl^-)/fluconazole in starting materials. According to the molecular formula of complexes 1–6, the

Table 5
Selected bond lengths (Å) and angles (deg) for complex 4

<i>Bond lengths</i>			
Ni(1)–N(6)#1	2.007(2)	Ni(1)–N(6)#2	2.007(2)
Ni(1)–N(3)	2.025(2)	Ni(1)–N(3)#3	2.025(2)
Ni(1)–O(2)#3	2.389(2)	Ni(1)–O(2)	2.389(2)
Ni(2)–N(12)#4	2.018(2)	Ni(2)–N(12)#5	2.018(2)
Ni(2)–N(9)#6	2.022(2)	Ni(2)–N(9)	2.022(2)
Ni(2)–O(4)#6	2.396(2)	Ni(2)–O(4)	2.396(2)
<i>Bond angles</i>			
N(6)#1–Ni(1)–N(6)#2	180.0	N(6)#1–Ni(1)–N(3)	88.67(9)
N(6)#2–Ni(1)–N(3)	91.33(9)	N(9)#6–Ni(2)–O(4)	89.43(8)
N(12)#4–Ni(2)–N(12)#5	180.0	N(12)#4–Ni(2)–O(4)#6	89.59(9)
C(7)–N(6)–Ni(1)#7	129.2(2)	C(20)–N(12)–Ni(2)#8	128.2(2)
C(5)–N(3)–Ni(1)	126.12(19)	C(18)–N(9)–Ni(2)	129.90(19)

Symmetry transformations used to generate equivalent atoms: #1 $x, -y + 3/2, z - 1/2$; #2 $-x + 2, y - 1/2, -z + 3/2$; #3 $-x + 2, -y + 1, -z + 1$; #4 $x, -y + 3/2, z + 1/2$; #5 $-x + 1, y - 1/2, -z + 1/2$; #6 $-x + 1, -y + 1, -z + 1$; #7 $-x + 2, y + 1/2, -z + 3/2$; #8 $-x + 1, y + 1/2, -z + 1/2$.

Table 6
Selected bond lengths (Å) and angles (deg) for complex 5

<i>Bond lengths</i>			
Ni(1)–N(6)#1	2.133(3)	Ni(1)–N(6)#2	2.133(3)
Ni(1)–N(3)#3	2.145(3)	Ni(1)–N(3)	2.145(3)
Ni(1)–Cl(1)	2.5246(10)	Ni(1)–Cl(1)#3	2.5246(10)
<i>Bond angles</i>			
N(6)#1–Ni(1)–N(6)#2	180.00(12)	N(6)#1–Ni(1)–N(3)#3	88.86(11)
N(6)#2–Ni(1)–N(3)#3	91.14(11)	N(3)–Ni(1)–Cl(1)	90.00(8)
N(6)#1–Ni(1)–Cl(1)	90.54(8)	N(6)#2–Ni(1)–Cl(1)	89.46(8)
Cl(1)–Ni(1)–Cl(1)#3	180.00(4)	C(5)–N(3)–Ni(1)	129.6(2)
C(4)–N(3)–Ni(1)	127.2(3)	C(6)–N(6)–Ni(1)#4	132.1(2)

Symmetry transformations used to generate equivalent atoms: #1 $x, -y + 1, z - 1/2$; #2 $-x + 1/2, y + 1/2, -z + 1/2$; #3 $-x + 1/2, -y + 3/2, -z$; #4 $-x + 1/2, y - 1/2, -z + 1/2$.

Table 7
Selected bond lengths (Å) and angles (deg) for complex 6

<i>Bond lengths</i>			
Mo(1)–O(3)#1	1.736(3)	Mo(1)–O(3)	1.736(3)
Mo(1)–O(2)#1	1.757(2)	Mo(1)–O(2)	1.757(2)
Ni(1)–O(2)#2	2.005(2)	Ni(1)–O(2)	2.005(2)
Ni(1)–N(3)	2.112(3)	Ni(1)–N(3)#2	2.112(3)
Ni(1)–N(6)#3	2.126(3)	Ni(1)–N(6)#4	2.126(3)
<i>Bond angles</i>			
O(3)#1–Mo(1)–O(3)	111.0(3)	O(3)#1–Mo(1)–O(2)	108.41(14)
O(3)–Mo(1)–O(2)#1	108.41(14)	O(3)#1–Mo(1)–O(2)#1	109.71(15)
O(2)#2–Ni(1)–O(2)	180.0(2)	O(2)#2–Ni(1)–N(3)	88.10(11)
N(3)#2–Ni(1)–N(6)#4	87.61(10)	N(6)#3–Ni(1)–N(6)#4	180.0(2)
C(6)–N(6)–Ni(1)#5	131.2(2)	Mo(1)–O(2)–Ni(1)	158.11(16)

Symmetry transformations used to generate equivalent atoms: #1 $-x + 1, y, -z - 1/2$; #2 $-x + 1, -y, -z$; #3 $x - 1/2, -y + 1/2, z - 1/2$; #4 $-x + 3/2, y - 1/2, -z + 1/2$; #5 $-x + 3/2, y + 1/2, -z + 1/2$.

stoichiometric ratio of Ni(II) (or anions)/fluconazole in complexes 1–6 is 1:1 or 1:2. The experimental data and stoichiometric ratio show that both Ni(II) and anions in

starting materials are in excess with respect to fluconazole and it is ensured that fluconazole can be transformed as possible as totally in the self-assembly of the six compounds. Interestingly, in the synthesis of complex **6**, both the molar ratio of MoO_4^{2-} /fluconazole and that of Cl^- /fluconazole are 2:1 in starting materials, but only MoO_4^{2-} has entered into the crystalline phase of complex **6**.

3.2. Description of crystal structures

3.2.1. Crystal structure of $(\text{C}_{13}\text{H}_{11}\text{N}_6\text{OF}_2)_2\text{Ni}_2(\text{NO}_3)_2$ (**1**)

DMF, as a polar aprotic solvent, possesses superior solvent power. When $\text{Ni}(\text{NO}_3)_2$ and DMF were utilized, a molecular binuclear nickel cluster $(\text{C}_{13}\text{H}_{11}\text{N}_6\text{OF}_2)_2\text{Ni}_2(\text{NO}_3)_2$ (**1**) was obtained (Fig. 1). Complex **1** crystallizes in *Pbca* space group, with one Ni(II), one fluconazole and one bidentate-coordinated NO_3^- in the asymmetric unit. The Ni(II) center exhibits a distorted octahedral geometry and is six coordinated by two nitrogen atoms and four oxygen atoms. The nitrogen atoms are from two triazole ligands of two fluconazole. Two oxygen atoms are from one NO_3^- and another two oxygen atoms are from two hydroxyl groups of two fluconazole. Complex **1** consists of two symmetrical fluconazole, each of which links two Ni(II) centers via its deprotonated hydroxyl group and two triazole ligands. The Ni...Ni distance is 3.048 Å and the

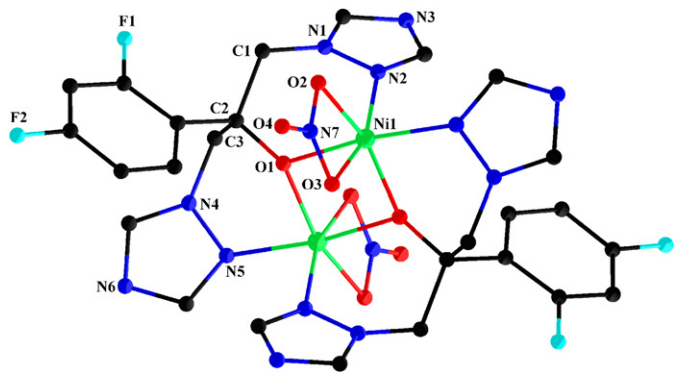


Fig. 1. Binuclear nickel cluster of complex **1** (H atoms omitted for clarity).

dihedral angle of the two triazole planes in one fluconazole is 57.9° .

3.2.2. Crystal structure of $(\text{C}_{13}\text{H}_{12}\text{N}_6\text{OF}_2)_2\text{Ni}(\text{NO}_3)_2 \cdot \text{H}_2\text{O}$ (**2**)

In the construction of metal–organic polymers, solvent effect has received much attention [9]. If protic solvent such as water was utilized instead of DMF in the preparation of complex **1**, a new complex $(\text{C}_{13}\text{H}_{12}\text{N}_6\text{OF}_2)_2\text{Ni}(\text{NO}_3)_2 \cdot \text{H}_2\text{O}$ (**2**) was obtained. Complex **2** crystallizes in *C2/c* space group, its asymmetric unit is similar to that in complex **1** except containing an additional dissociated water. The Ni(II) center is coordinated by four nitrogen atoms from four fluconazole and two oxygen atoms from two NO_3^- to furnish an octahedral geometry. Each fluconazole links two Ni(II) centers via its two triazole ligands, leaving the hydroxyl group uncoordinated. The Ni...Ni distance is 10.356 Å and the dihedral angle between the two triazole planes in one fluconazole is 91.2° . The Ni(II) centers are bridged by double-stranded fluconazole and complex **2** exhibits a one-dimensional (1D) chain-like structure (Fig. 2).

The NO_3^- in complex **2** exhibits monodentate coordination mode (Fig. 2) and the Ni–O distance (2.427 Å) (Table 3) is much longer than that in complex **1** (Ni(1)–O(2): 2.1261(16) Å, Ni(1)–O(3) 2.1548(18) Å) (Table 2), which indicates that the binding strength of NO_3^- anion in polar protic solvent (water) is weaker than that in polar aprotic solvent (DMF). Interestingly, on heating complex **2** in DMF under reaction conditions (sealed in Teflon-lined autoclaves and heated at 110°C for 3 days), we can obtain complex **1**, as evidenced by the powder XRD pattern of the product, which is in good accordance with the simulated XRD powder pattern of complex **1** (see Fig. S1 in the supporting information). However, heating complex **1** in water can not give complex **2**. The irreversible conversion between complexes **1** and **2** indicated that complex **1** is more thermodynamic stable than complex **2**. Actually, the edge-sharing binuclear nickel clusters are common in biological system [10], maybe it is due to their thermodynamic stability.

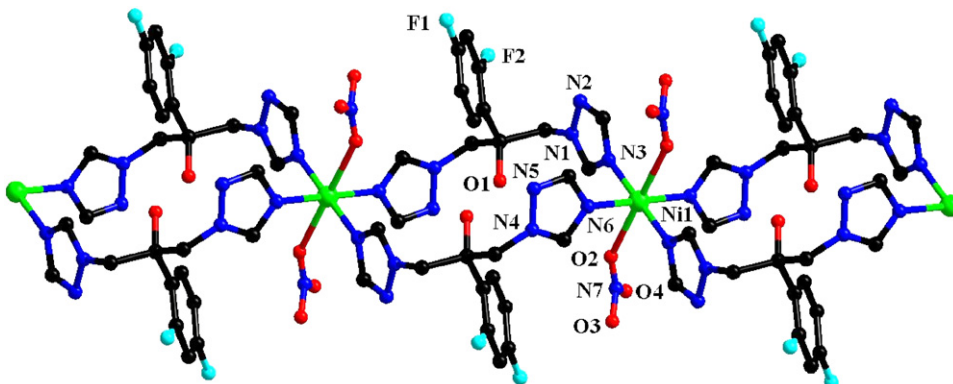


Fig. 2. 1D chain-like structure of complex **2** (H atoms and dissociated water omitted for clarity).

3.2.3. Crystal structure of $(C_{13}H_{12}N_6OF_2)Ni(SO_4)(DMF)_2(H_2O)$ (**3**)

In order to investigate the effect of anionic size on the structural motif, a bigger anion such as SO_4^{2-} is chosen. When $NiSO_4$ was utilized as starting material instead of $Ni(NO_3)_2$ in the preparation of complex **1**, a novel complex $(C_{13}H_{12}N_6OF_2)Ni(SO_4)(DMF)_2(H_2O)$ (**3**) was obtained. Complex **3** crystallizes in $P2_1/c$ space group, its asymmetric unit contains one Ni(II), one fluconazole, one SO_4^{2-} , one coordinated water, one coordinated DMF and one dissociated DMF.

The Ni(II) center in complex **3** exhibits a distorted octahedral geometry and is six coordinated by one aqua ligand, one DMF, two nitrogen atoms from two fluconazole, and two oxygen atoms from two SO_4^{2-} . Each fluconazole links two Ni(II) centers ($Ni \cdots Ni$ distance: 10.794 Å) via its two triazole ligands (dihedral angle: 80.4°), leaving the hydroxyl group uncoordinated. One SO_4^{2-} links two Ni(II) centers with the $Ni \cdots Ni$ distance of 4.937 Å. Thus, 1D chains constructed by double stranded fluconazole-bridge and double stranded SO_4^{2-} -bridge are observed

in complex **3** (Fig. 3). SO_4^{2-} , as a good H-bond acceptor, can be coordinated to metal center, however, such double-stranded SO_4^{2-} -bridge is rarely reported in previous work.

3.2.4. Crystal structure of $(C_{13}H_{12}N_6OF_2)_2Ni(H_2O)_2(SO_4) \cdot 4H_2O$ (**4**)

If water was utilized as solvent instead of DMF in the preparation of complex **3**, another novel complex $(C_{13}H_{12}N_6OF_2)_2Ni(H_2O)_2(SO_4) \cdot 4H_2O$ (**4**) was obtained. Complex **4** crystallizes in $P2_1/c$ space group, its asymmetric unit contains two Ni(II), two fluconazole, two coordinated water, one dissociated SO_4^{2-} and four dissociated water. Two crystallographically unique Ni(II) exhibit similar octahedral coordination spheres, each of them is six coordinated by two aqua ligands and four nitrogen atoms from four fluconazole. Complex **4** exhibits a two-dimensional (2D) parquet motif with a uniform (4, 4) net topology (Fig. 4). The two crystallographically unique metal centers, Ni(1) (position coordinates: 1.000, 0.500,

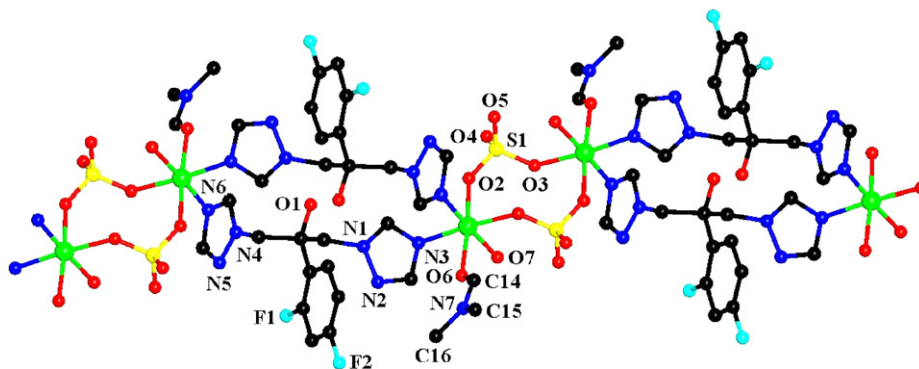


Fig. 3. 1D chain bridged by two stranded SO_4^{2-} and fluconazole in complex **3** (H atoms and dissociated DMF omitted for clarity).

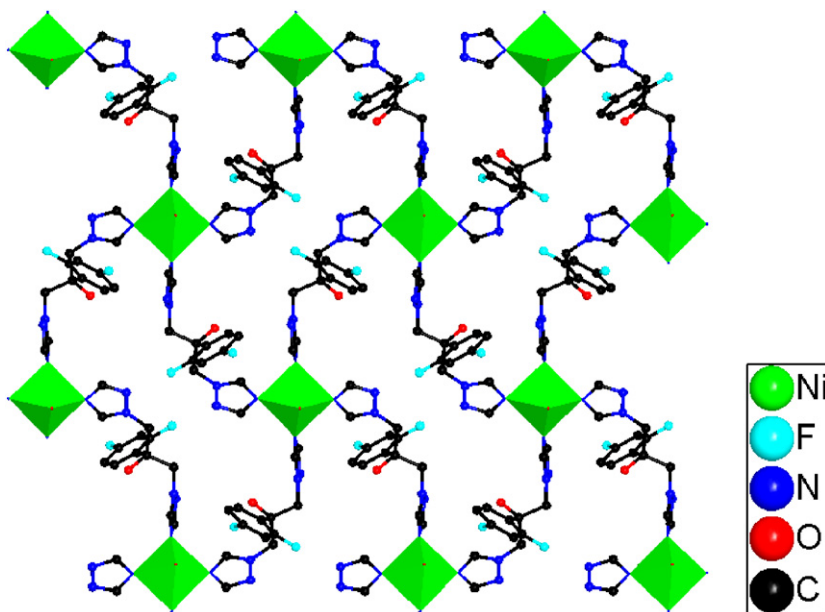


Fig. 4. 2D structure of complex **4** (H atoms, dissociated SO_4^{2-} and water omitted for clarity).

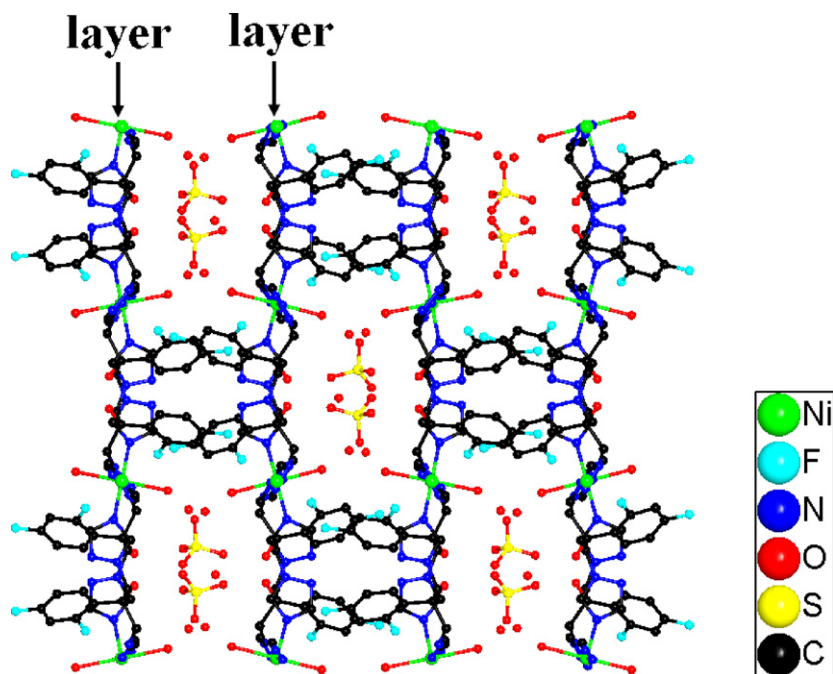


Fig. 5. 3D porous framework of complex 4 and guest SO₄²⁻ anions and water molecules occupy the channel (H atoms omitted for clarity).

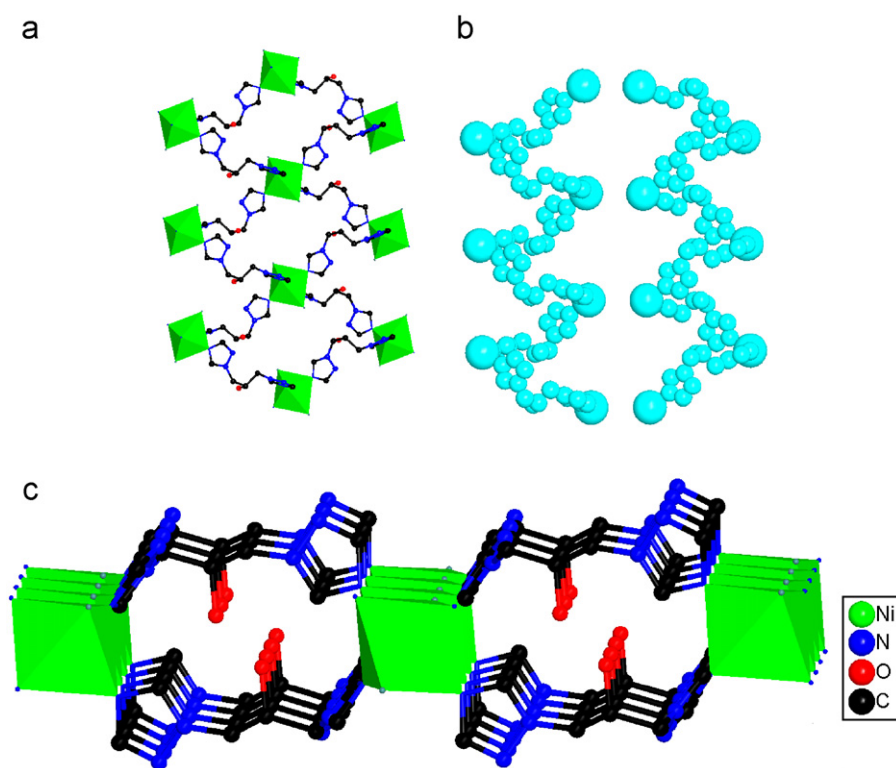


Fig. 6. 2D framework of complex 5, which is constructed by alternating left and right-handed helices: (a) side-view; (b) top-view; (c) space filling diagrams of the isolated right-handed and left-handed helices (H, Cl⁻ atoms, 2,4-difluorophenyl group of fluconazole and methanol molecules omitted for clarity).

0.500) and Ni(2) (position coordinates: 0.500, 0.500, 0.500) are located in two neighboring layers. The neighboring Ni(1)⋯Ni(1A) and Ni(2)⋯Ni(2A) distances are the same (11.077 Å). The dihedral angles between the two triazole planes of the two crystallographically unique fluconazole

are 79.6° and 89.4°, respectively. The 2,4-difluorophenyl ligands of fluconazole orient above or below each layer and there is not strong π - π stacking interactions between the aromatic groups because the centroid-centroid distance is no shorter than 4.3 Å. However, weak interactions exist

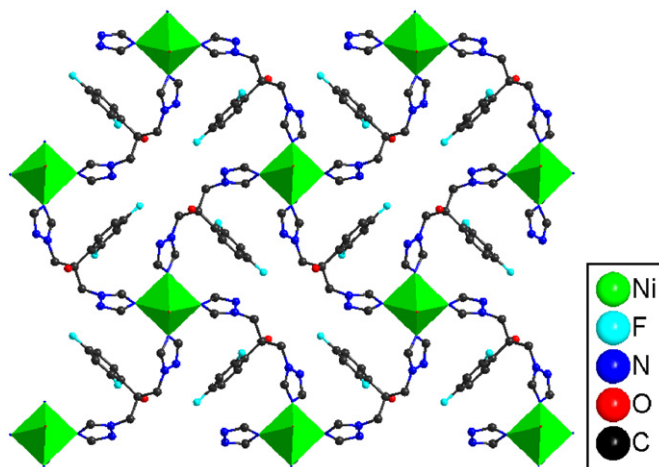


Fig. 7. 2D structure of complex **6** with the phenyl rings of fluconazole orderly array within the layer (H, Mo atoms, and dissociated water omitted for clarity).

between the F atom of phenyl ligand and the O atom in the neighboring layers, for example, the F4...O2A distance is 3.350 Å (atom with additional label A refers to the symmetry operation: $1-x, -0.5+y, 0.5-z$). Complex **4** exhibits a three-dimensional (3D) porous architecture and the channels are occupied by the dissociated SO_4^{2-} and water molecules (Fig. 5). Calculated by PLATON software, the channel is ca. 472 \AA^3 per unit cell. Weak interactions also exist between the SO_4^{2-} and the neighboring layers, for example, the O5...O2B, O5...O4, O6...O1C distances are 2.734, 2.775, 2.790 Å, respectively (atom with additional labels B and C refer to the symmetry operations: B $x-1, y, z$; C $x-1, 1.5-y, -0.5+z$). The shorter O...O distances (less than 2.8 Å) indicate that SO_4^{2-} (guest) plays an important role in stabilizing the porous framework of complex **4**. Thus it is presumed that the porosity is not permanent and it is closely related with the guests.

The SO_4^{2-} in complex **4** is uncoordinated, whereas in complex **3**, SO_4^{2-} anion covalently bridges two Ni(II) centers (Ni(1)–O(2): 2.065(3) Å, Ni(1)–O(3)#1, 2.089(3) Å) (Table 4). It is indicated that the binding strength of SO_4^{2-} anion in water is much weaker than that in DMF [11]. It is inferred that solvents will influence the properties of the anions, thus change the network of the product. Different from complexes **1** and **2**, complexes **3** and **4** can not be interconverted under similar reaction conditions if change the species of solvent.

3.2.5. Crystal structure of $(\text{C}_{13}\text{H}_{12}\text{N}_6\text{OF}_2)_2\text{NiCl}_2 \cdot 2(\text{CH}_3\text{OH})$ (**5**)

In an attempt to explore the effect of a smaller anion on the self-assembly of Ni(II)–fluconazole complex, Cl^- was chosen in our experiment. When NiCl_2 and methanol were utilized as starting materials, a complex $(\text{C}_{13}\text{H}_{12}\text{N}_6\text{OF}_2)_2\text{NiCl}_2 \cdot 2(\text{CH}_3\text{OH})$ (**5**) is obtained. Complex **5** crystallizes in $C2/c$ space group, its asymmetric unit contains one Ni (II), one fluconazole, one Cl^- and one dissociated methanol molecule. The Ni(II) center exhibits a distorted octahedral

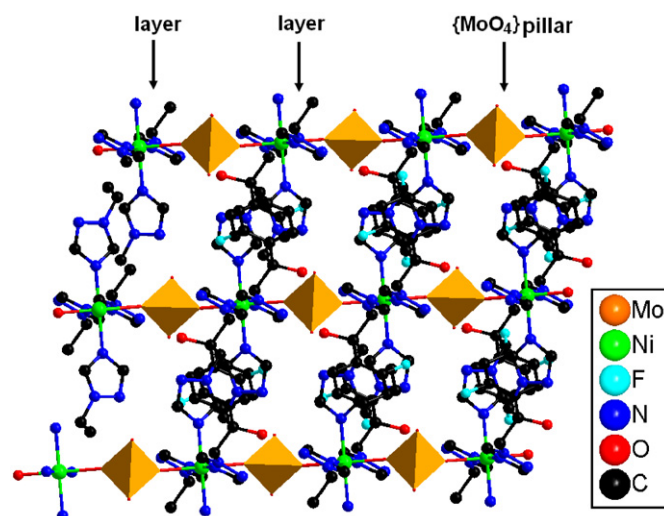


Fig. 8. 2D layers pillared by $\{\text{MoO}_4\}$ tetrahedra to construct a 3D architecture in complex **6** (H atoms and dissociated water omitted for clarity).

geometry and is six coordinated by two Cl^- and four nitrogen atoms from four fluconazole. Each fluconazole links two Ni(II) centers (Ni...Ni distances: 11.096 and 9.288 Å) via its two triazole ligands (dihedral angle: 74.5°), leaving the hydroxyl group uncoordinated. A 2D framework is observed in complex **5**. However, the layer is completely different from that in complex **4**, it is composed of alternating left- and right-handed helices with a pitch of 18.576 Å (Fig. 6). Interestingly, the top-view (Fig. 6b) of the layer exhibits a 1D chain, which is similar to that observed in complex **2**.

3.2.6. Crystal structure of $(\text{C}_{13}\text{H}_{12}\text{N}_6\text{OF}_2)_4\text{Ni}_2(\text{MoO}_4)_2 \cdot 6\text{H}_2\text{O}$ (**6**)

In an attempt to construct a 3D network in which anion can act as bridging ligand, an anion with suitable size

should be considered. When the starting material is the mixture of NiCl_2 (0.5 mmol), $\text{Na}_2\text{MoO}_4 \cdot 2\text{H}_2\text{O}$ (1 mmol), fluconazole (0.5 mmol) and water (10 mL), a novel coordination polymer $(\text{C}_{13}\text{H}_{12}\text{N}_6\text{OF}_2)_4\text{Ni}_2(\text{MoO}_4)_2 \cdot 6\text{H}_2\text{O}$ (**6**) is obtained. Complex **6** crystallizes in $C2/c$ space group. The ratio of the crystallographically unique Ni(II), fluconazole, MoO_4^- and dissociated water molecule is 1:1:0.5:2. One dissociated water has two positions owing to the crystallographic disorder of O(5) and O(5A). Each of them has 50% occupancy over the two positions. The Ni(II) center exhibits a distorted octahedral geometry and is six coordinated by two MoO_4^- and four nitrogen atoms from four fluconazole. Each fluconazole links two Ni(II) centers (Ni...Ni distance: 11.507 Å) via its two triazole

ligands (dihedral angle: 116.5°), leaving the hydroxyl group uncoordinated. The Ni(II) centers are linked by fluconazole to form a 2D parquet motif with a uniform (4, 4) net topology (Fig. 7). However, different from the layers in complex **4**, the 2,4-difluorophenyl ligands of fluconazole aren't above or below the layer, but orderly array within the layer. There are not weak interactions between the F atoms and O atoms in the neighboring layers. The centroid–centroid distance of two neighboring phenyl rings is no shorter than 4.2 Å, and no strong π – π stacking interactions exist.

Each MoO_4^- anion links two Ni(II) centers via its two oxygen atoms, leaving another two oxygen atoms uncoordinated. Complex **6** exhibits a 3D architecture, in which the

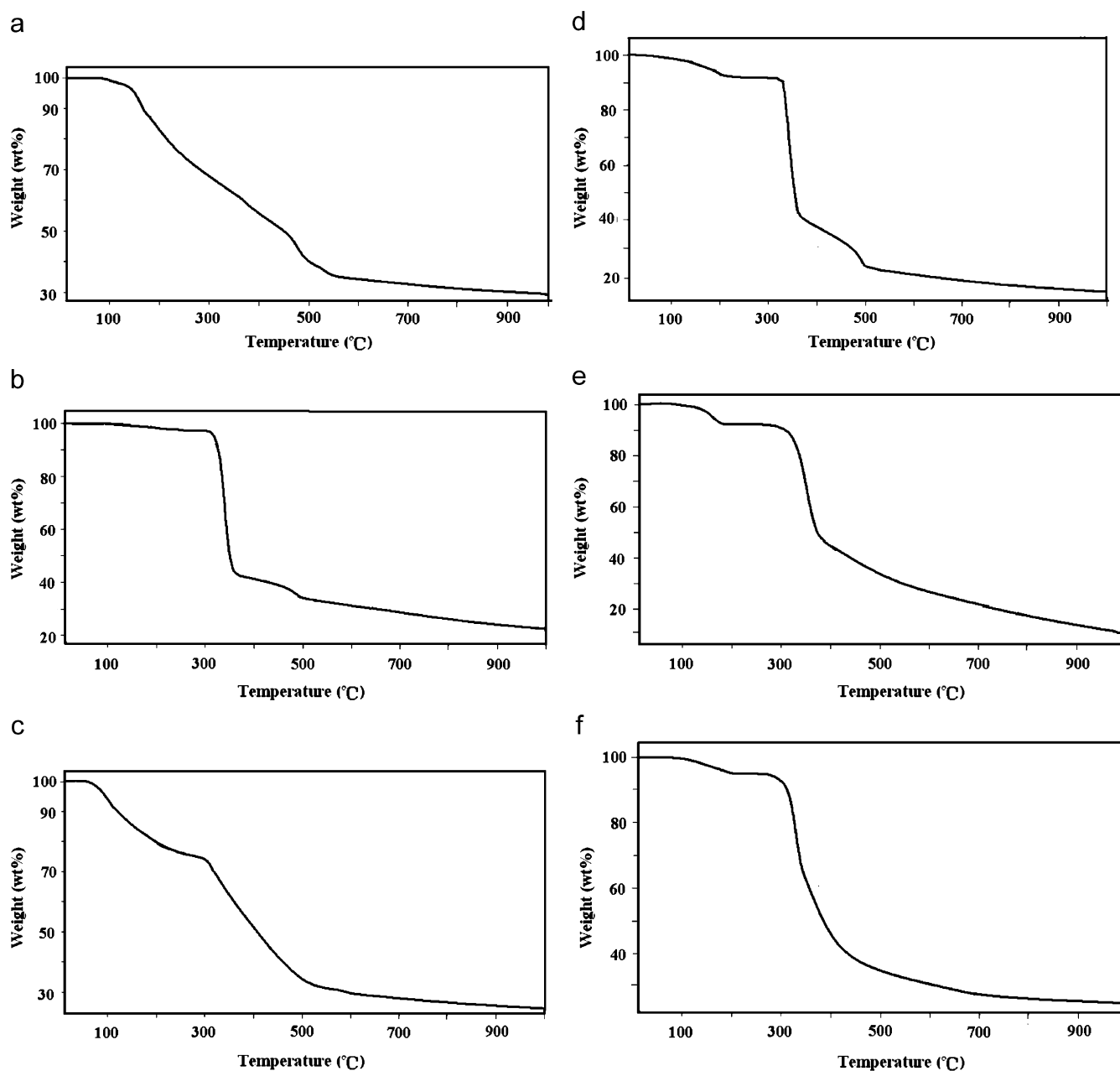


Fig. 9. TG curves for compounds 1 (a), 2 (b), 3 (b), 4 (d), 5 (e) and 6 (f).

2D layers are pillared by $\{\text{MoO}_4\}$ tetrahedra (Fig. 8). Dissociated water molecules occupied the cavities. Calculated by PLATON software, the cavity is ca. 83 \AA^3 per unit cell. The porosity of complex **6** is more stable than that of complex **4** because the interlayer interactions are covalent bonds. It is rarely reported that MoO_4^- anion acts as covalently bridging ligand [12], the present work shows it is possible when MoO_4^- meets the size of pillar.

3.3. TG analysis

The TG analyses of the six compounds are performed in the temperature range of 20–1000 °C. From 100 to 1000 °C, compound **1** gradually loses its weight and the total weight loss is 70.72% (calculated value: 71.60%), corresponding to the oxidization and decomposition of fluconazole (Fig. 9a).

From about 120 to 310 °C, compound **2** loses its crystal water, the weight loss is 2.30%, in good accordance with the calculated value (2.21%). From 310 to 1000 °C, the weight loss is 75.20% (calculated value: 75.28%), corresponding to the oxidization and decomposition of fluconazole (Fig. 9b).

In the range of 50–300 °C, compound **3** loses its crystal and coordinated solvent molecules (DMF and water), the weight loss of this step is 26.05%, in good accordance with the calculated value (26.24%). From 300 to 1000 °C, the TG curve of **3** exhibits steady weight losses, which corresponds to the oxidization and decomposition of fluconazole (Fig. 9c). The total weight loss of **3** is 75.40%, in good accordance with the calculated value (75.20%).

From room temperature to 320 °C, compound **4** loses its crystal water, the weight loss is 8.45%, in good accordance with the calculated value (8.23%). From 320 to 1000 °C, the weight loss is 74.27% (calculated value: 74.05%), corresponding to the loss of the coordinated water and the oxidization and decomposition of fluconazole (Fig. 9d).

From room temperature to 310 °C, compound **5** loses its crystal methanol molecules, the weight loss of this step is 8.05%, in good accordance with the calculated value (7.94%). From 310 to 1000 °C, the TG curve of **5** exhibits steady weight losses, which corresponds to the loss of chlorine and the oxidization and decomposition of fluconazole (Fig. 9e). The total weight loss of **5** is 90.10%, in good accordance with the calculated value (90.69%).

Compound **6** loses its crystal water in the range of 100–300 °C, the weight loss of this step is 5.95%, in good accordance with the calculated value (6.10%). From 300 to 1000 °C, the weight loss of **6** is 69.80% (calculated value: 69.15%), which corresponds to the oxidization and decomposition of fluconazole (Fig. 9f).

3.4. Magnetic property

The variable temperature magnetic susceptibility data of compounds **1**, **3** and **6** were measured in the temperature

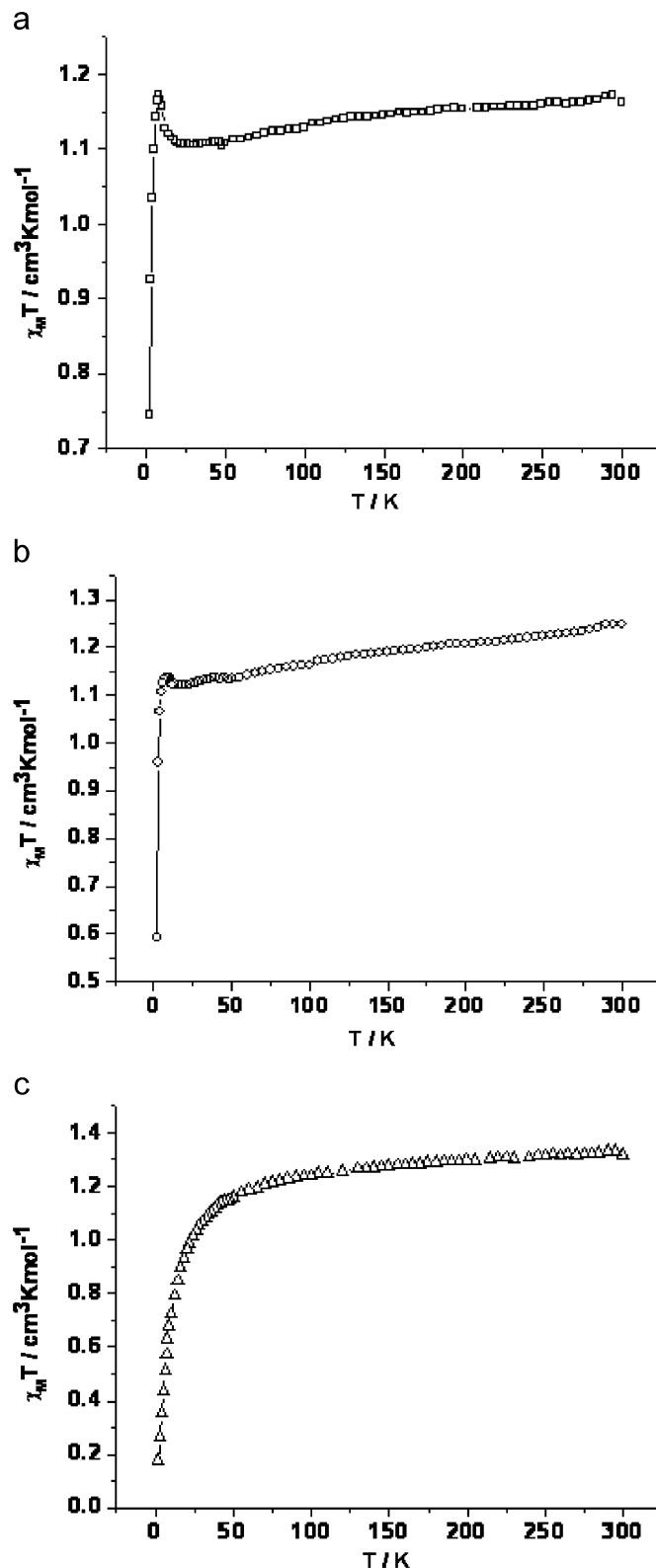


Fig. 10. The magnetic susceptibility of compounds **1** (a), **3**(b) and **6** (c).

range 2–300 K under 1 kOe. As for complex **1**, the χ^{-1} versus T is nearly a straight line above 30 K (Fig. 10a), which it obeys the Curie–Weiss law. The Curie and Weiss

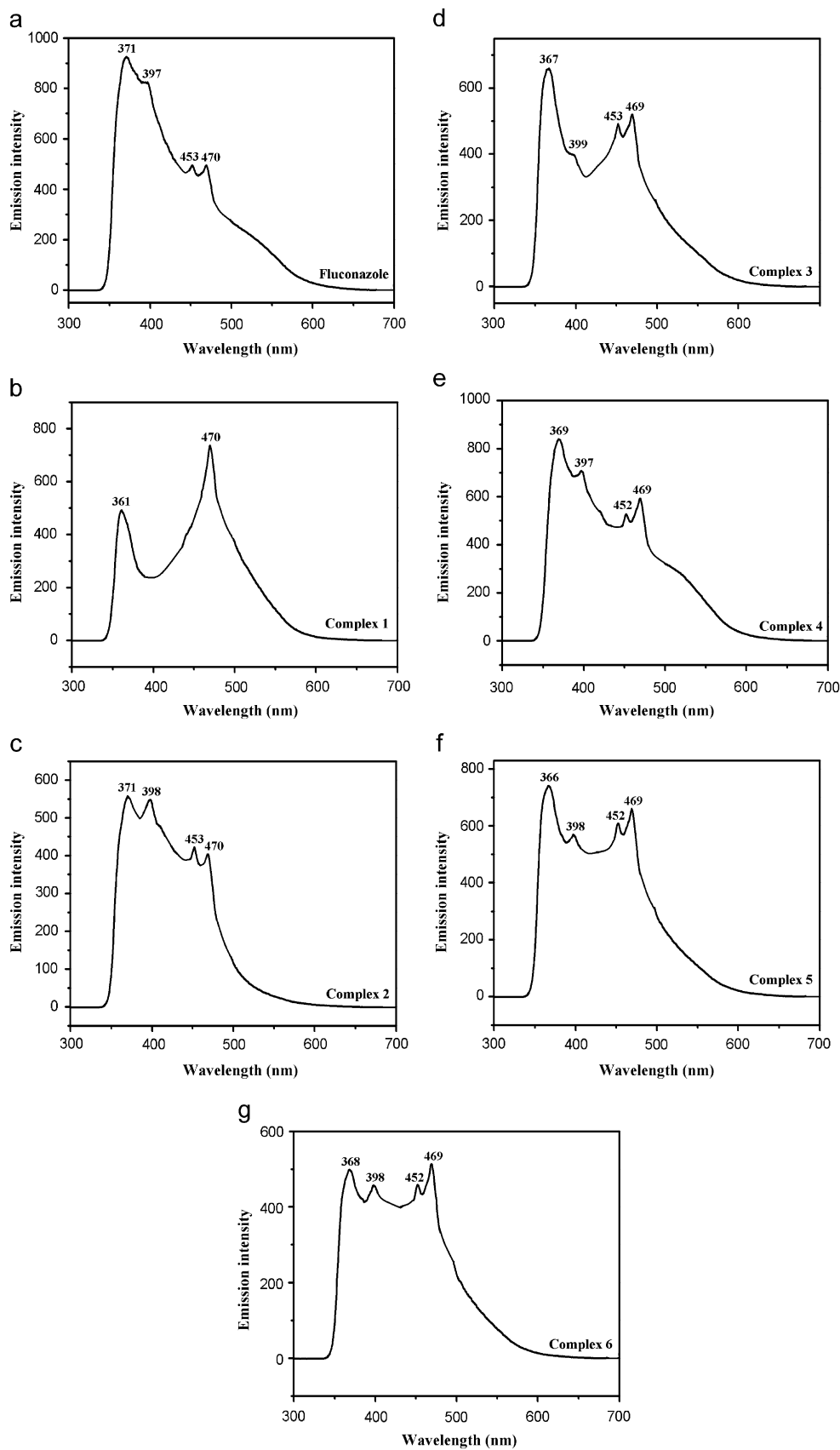
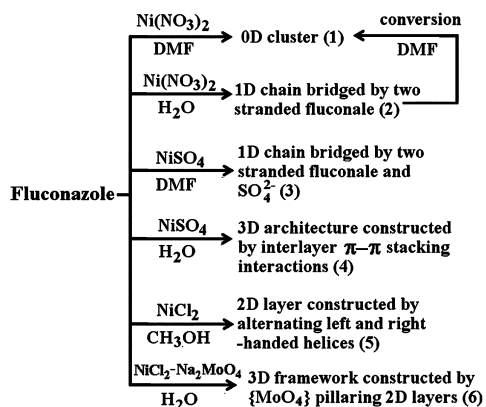


Fig. 11. Solid-state emission spectra at room temperature of fluconazole (a), complex 1 (b), complex 2 (c), complex 3 (d), complex 4 (e), complex 5 (f), complex 6 (g).



Scheme 2. Anion-directed self-assembly.

constants, C and θ are $1.18 \text{ cm}^3 \text{ K mol}^{-1}$ and -4.24 K , respectively, based on the equation $\chi^{-1} = C/(T-\theta)$. The negative Weiss constant indicates an overall intramolecular weakly antiferromagnetic interaction between the nickel(II) ions. At low temperature, the $\chi_{\text{M}}T$ increasing maybe caused by zero splitting and magnetic anisotropy.

The variable temperature magnetic susceptibility data for complex **3** is similar to complex **1** (Fig. 10b). However, C and θ are $1.26 \text{ cm}^3 \text{ K mol}^{-1}$ and -8.77 K , respectively, indicating an overall intramolecular antiferromagnetic interaction between the nickel(II) ions. The magnetic coupling between nickel(II) through the ligand and inter-chain can be ignored for the long distance ($> 10.794 \text{ \AA}$).

Complex **6** shows an antiferromagnetic interaction between the nickel (II) ions. Magnetic data for the compound is plotted in Fig. 10c. The $\chi_{\text{M}}T$ value of complex **6** smoothly decreases as the temperature is lowered, attains about 70 K and quickly decreases in the lower temperature region. According to the structural data, nickel (II) ions are separated by fluconazole and the magnetic coupling is very weak, the magnetic properties are similar to single ions behavior.

3.5. Photoluminescence property

The powder X-ray diffraction patterns of complexes **1–6** are shown in Fig. S2 in the supporting information. All the peaks of the six complexes can be indexed to their respective simulated XRD powder pattern, which indicates each of the six complexes is pure phase. The emission spectra of fluconazole and complexes **1–6** in the solid state ($\lambda_{\text{ex}} = 310 \text{ nm}$) at room temperature are depicted in Fig. 11. As shown in Fig. 11a, fluconazole displays one intense emission peak at 371 nm and three weak shoulder peaks at 397 , 453 , 470 nm , they are attributable to different intra-ligand transitions of fluconazole, such as $\pi \rightarrow \pi^*$, $\pi^* \rightarrow n$, $n \rightarrow n^*$, $\pi \rightarrow n$ transitions [13]. In the emission spectra of complex **1**, the weak shoulder peaks at 397 and 453 nm of discrete fluconazole disappear, whereas the peak of 470 nm appears as the maximum emission peak (Fig. 11b). The

emission at 361 nm of complex **1**, which is different from that of discrete fluconazole, might be the ligand-to-metal charge transfer (LMCT) [14]. It is indicated that the hydroxyl group and triazole ligand of fluconazole coordinated to Ni(II) center plays an important role in the photoluminescence property of complex **1**.

However, the emission spectra of complexes **2–6** are somewhat similar to that of the discrete fluconazole, that is to say, the four emission peaks of discrete fluconazole still appear although some peaks shift a little, which may be due to the uncoordinated hydroxyl group in complexes **2–6** compared with the coordinated ligands in complex **1** [13,14b]. Interestingly, it is found that the relative intensities of the four peaks in the emission spectra of complexes **2–6** are different (Fig. 11c–g), which indicates that the intra-ligand transitions of fluconazole have been enhanced or weakened to different extent due to the introduction of different anions and the different structures of complexes. The detailed mechanism is under investigation. Such phenomenon is rarely reported in previous work [15] and the difference of photoluminescence between the organic ligand and the metal–organic complex is usually caused by the metal ion-involved charge transfer, such as LMCT [13,14], but not by the intra-ligand transition.

4. Conclusion

In conclusion, using fluconazole and Ni (II) salts, six anion-directed self-assemblies have been synthesized with their structures spanning zero, one, two and three dimensions (Scheme 2). Complex **2** can be irreversibly converted to complex **1** in the presence of DMF. The photoluminescence properties of complexes **1–6** indicate that the introduction of different anions can lead to different structures of Ni(II)-complexes, and thus enhance or weaken the intra-ligand transitions of fluconazole.

As well known, the interaction of metal ions with drugs would influence the activities of drugs. The metal oxidation state, the type and number of donor atoms, as well as their relative disposition within the ligand are major factors determining structural and activity relationship [7,8]. However, so far the effect of anion on the property of drug is still unexplored. The field is firstly investigated in the present work and it is indicated that the anions can influence the photoluminescence property of drug.

Owing to the variety of anions, further research can focus on the introduction of various kinds of anions with different functions into the metal–fluconazole complexes, such as N_3^- , polyanions. It is under investigation now.

Acknowledgments

This work was supported by the National Natural Science Foundation of China (No. 20331010), and the Natural Science Foundation Project of Chongqing (No. CSTC/ 2006BB4178).

Appendix A. Supporting information

Supplementary data associated with this article can be found in the online version at doi:10.1016/j.jssc.2007.01.036.

References

- [1] (a) P. Molenveld, S. Kapsabelis, J.F.J. Engbersen, D.N. Reinhoudt, *Chem. Rev.* 119 (1997) 2948;
(b) F.P. Schmidtchen, M. Berger, *Chem. Rev.* 97 (1997) 1609.
- [2] (a) P.D. Beer, *Chem. Commun.* (1996) 689;
(b) W. Xu, J.J. Vittal, R.J. Puddephatt, *Chem. Commun.* 117 (1995) 8362;
(c) A. Bianchi, E. García-España, K. Bowman-James, *Supramolecular Chemistry of Anions*, Wiley-VCH, Weinheim, 1997, pp. 1–30.
- [3] (a) H.J. Kim, W.C. Zin, M. Lee, *J. Am. Chem. Soc.* 126 (2004) 7009;
(b) S.J. Coles, J.G. Frey, P.A. Gale, M.B. Hursthouse, M.E. Light, K. Navakhun, G.L. Thomas, *Chem. Commun.* (2003) 1462;
(c) P.A. Gale, *Coord. Chem. Rev.* 240 (2003) 191;
(d) R. Vilar, *Angew. Chem. Int. Ed.* 42 (2003) 1460;
(e) J.L. Atwood, A. Szumna, *Chem. Commun.* (2003) 940;
(f) M. Schweiger, S.R. Seidel, A.M. Arif, P.J. Stang, *Inorg. Chem.* 41 (2002) 2556;
(g) P.A. Gale, *Coord. Chem. Rev.* 213 (2001) 79;
(h) S.T. Cheng, E. Doxiadi, R. Vilar, A.J.P. White, D.J. Williams, *Dalton Trans.* (2001) 2239;
(i) P.D. Beer, P.A. Gale, *Angew. Chem. Int. Ed.* 40 (2001) 486 (and references therein);
(j) P.A. Gale, *Coord. Chem. Rev.* 199 (2000) 181;
(k) R. Vilar, D.M.P. Mingos, A.J.P. White, D.J. Williams, *Angew. Chem. Int. Ed.* 37 (1998) 1258;
(l) P.D. Beer, *Acc. Chem. Res.* 31 (1998) 71.
- [4] F. Diederich, P.J. Stang, *Templated Organic Synthesis*, Wiley-VCH, Weinheim, 2000, pp. 50–85.
- [5] B.A. Moyer, P.V. Bonnesen, *Supramolecular Chemistry of Anions*, Wiley-VCH, Weinheim, 1997.
- [6] A.E. Heald, G.M. Cox, W.A. Schell, J.A. Barlett, J.A. Perfect, *AIDS* 10 (1996) 263.
- [7] (a) R.J. Sunberg, R.B. Martin, *Chem. Rev.* 74 (1974) 471;
(b) M.A. Ali, A.H. Mirza, M. Nazimuddin, P.K. Dhar, R.J. Butcher, *Trans. Met. Chem.* 27 (2002) 27.
- [8] (a) N.M. Agh-Atabay, B. Dulger, F. Gucin, *Eur. J. Med. Chem.* 38 (2003) 875;
(b) Y. Inoue, M. Hoshino, H. Takahashi, T. Noguchi, T. Murata, Y. Kanzaki, H. Hamashima, M. Sasatru, *J. Inorg. Biochem.* 92 (2002) 37;
(c) S.E. Castillo-Blum, N. Barba-Behrens, *Coord. Chem. Rev.* 196 (2000) 3;
(d) R.N. Patel, S. Kumar, K.B. Pandeya, *J. Inorg. Biochem.* 9 (2002) 61;
(e) A. Tavman, B. Ülküseven, N.M. Agh-Atabay, *Trans. Met. Chem.* 25 (2000) 324.
- [9] (a) T. Wu, D. Li, S.W. Ng, *Cryst. Eng. Commun.* 7 (2005) 514;
(b) M.A. Withersby, A.J. Blake, N.R. Champness, P.A. Cooke, P. Hubberstey, W.S. Li, M. Schroder, *Inorg. Chem.* 38 (1999) 2259.
- [10] (a) P. Amara, A. Volbeda, J.C. Fontecilla-Camps, M.J. Field, *J. Am. Chem. Soc.* 127 (2005) 2776;
(b) T.C. Harrop, M.M. Olmstead, P.K. Mascharak, *J. Am. Chem. Soc.* 126 (2004) 14714;
(c) S.J. George, J. Seravalli, S.W. Ragsdale, *J. Am. Chem. Soc.* 127 (2005) 13500.
- [11] A.A. Fedorov, D. Joseph-McCarthy, E. Fedorov, D. Sirakova, I. Graf, S.C. Almo, *Biochemistry* 35 (1996) 15962.
- [12] B. Moulton, M.J. Zaworotko, *Chem. Rev.* 101 (2001) 1629.
- [13] (a) W. Chen, J.Y. Wang, C. Chen, Q. Yue, H.M. Yuan, J.X. Chen, S.N. Wang, *Inorg. Chem.* 42 (2003) 944;
(b) M.S. Wang, G.C. Guo, M.L. Fu, L. Xu, L.Z. Cai, J.S. Huang, *Dalton Trans.* (2005) 2899;
(c) X.D. Chen, M. Du, T.C.W. Mak, *Chem. Commun.* (2005) 4417.
- [14] (a) L.Y. Zhang, G.F. Liu, S.L. Zheng, B.H. Ye, X.M. Zhang, X.M. Chen, *Eur. J. Inorg. Chem.* (2003) 2965;
(b) Z.Y. Fu, X.T. Wu, J.C. Dai, S.M. Hu, W.X. Du, H.H. Zhang, R.Q. Sun, *Eur. J. Inorg. Chem.* (2002) 2730.
- [15] Y. Gong, W. Tang, W.B. Hou, Z.Y. Zha, C.W. Hu, *Inorg. Chem.* 45 (2006) 4987.